ACS APPLIED MATERIALS & INTERFACES

RESEARCH ARTICLE

www.acsami.org

Electric Conductivity-Tunable Transparent Flexible Nanowire-Filled Polymer Composites: Orientation Control of Nanowires in a Magnetic Field

Takayuki Nagai, Nobuyuki Aoki, Yuichi Ochiai, and Katsuyoshi Hoshino*

Graduate School of Advanced Integrated Science, Chiba University, 1-33 Yayoi-cho, Inage-ku, Chiba 263-8522, Japan

Supporting Information

ABSTRACT: Cobalt compound nanowires were dispersed in a transparent nonconductive polymer film by merely stirring, and the film's transparency and electrical conductivity were examined. This composite film is a unique system in which the average length of the nanowires exceeds the film's thickness. Even in such a system, a percolation threshold existed for the electric conductivity in the direction of the film thickness, and the value was 0.18 vol%. The electric conductivity value changed from $\sim 1 \times 10^{-12}$ S/cm to $\sim 1 \times 10^{-3}$ S/cm when the volume fraction exceeded the threshold. The electric conductivity apparently followed the percolation model until the volume fraction of the nanowires was about 0.45 vol %. The visible light transmission and electric conductivity of the composite film of about 1 vol % nanowires were 92% and 5×10^{-3} S/cm, respectively. Moreover, the electric conductivity in the direction parallel to the film surface did not depend on the amount of the dispersed nanowires, and its value was about 1×10^{-14} S/cm. Even in a weak magnetic field of about 100 mT, the nanowires were aligned in a vertical and parallel direction to the film surface, and the electric conductivity of each aligned composite film was 2.0×10^{-2} S/cm and 2.1×10^{-12} S/cm. The relation between the average wire length and the electric conductivity was examined, and the effect of the magnetic alignment on that relation was also examined.

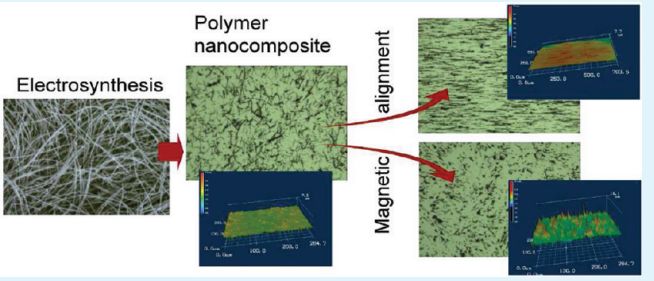

KEYWORDS: nanowire, cobalt compounds, percolation, transparent conductive film, magnetic alignment

1. INTRODUCTION

Transparent conductive materials are essential for the screen electrodes of flat-panel displays, such as liquid crystal devices (LCD), plasma displays (PDP), electronic papers (e-paper), and for the electrode materials of touch panels and solar cells. The most commonly used material is indium-tin-oxide (ITO).[1] Though this material has an extremely high transparency and electrical conductivity, indium, which is one of the constituent elements, is a rare metal, and its price is rapidly increasing because of the problem of limited resourcing. Moreover, its flexibility is insufficient because it is a ceramic, and therefore is not suitable for the next-generation flexible element, which can be freely rolled or bent.[2−5]

The development of transparent conductive materials, which satisfy the requirements, such as a high transparency and electrical conductivity, flexibility, low material cost, low processing cost for thin-film formation, and capability of manufacturing a large-area sheet, is now being promoted.[2] For instance, the following methods are being developed: dispersing carbon nanotubes in a transparent nonconductive polymer,[6−11] dispersing metal nanowires in a transparent nonconductive polymer,[12,13] developing a transparent electric conductive polymer,[14−19] forming a carbon nanotube-only network,[20−24] forming a metal nanowire-only network,[25,26] forming a metal nanomesh,[27,28] forming a graphene network,[29,30] forming a graphene oxides-dispersed single-walled carbon nanotube network,[31] forming ultrathin carbon coatings,[32] forming a layer-by-layer assembly of single-walled carbon nanotubes,[33] and forming a nanocomposite of a conductive polymer and metal oxide utilizing the corrosion reaction.[34,35] However, none of these methods satisfy all the previously mentioned requirements, thus the development of the materials and film production process is currently being carried out.

Recently, our group reported a method for manufacturing a large amount of cobalt compound nanowires (CCNWs) on the electrode substrate without using a template only by carrying out the electrolytic reduction of $[Co(NH_3)_6]^{3+}$ in an aqueous solution under standard temperature and pressure.[36] The obtained CCNW consisted of metallic cobalt, cobaltous hydroxide, and cobalt oxide, and its average diameter was 190 nm and the average length was 25 μm (applied electric charge: 1.0 C/cm^2).[36,37] We considered that a flexible sheet having a transparency and electric conductivity could be easily obtained by dispersing these CCNWs into a transparent nonconductive polymer solution and applying the dispersion liquid. Moreover, because the CCNW is a magnetic material, the CCNW can be aligned by applying a magnetic field. For instance, the development of an application for ACF

Received: March 2, 2011
Accepted: May 30, 2011
Published: May 30, 2011

(Anisotropic Conductive Film), etc., can be expected. Recently, it was found that the direction and position of a magnetic nanowire can be controlled by applying a magnetic field.[38−44] Also being studied is embedding nanowires into electronic devices such as field-effect-transistors,[38] UV sensors,[39] and temperature and humidity sensors[44] by a technique utilizing a magnetic field. However, there are few examples of applications for transparent conductive materials in which a metal nanowire is dispersed in a polymer to the best of our knowledge excluding the reports on Cu nanowires[12] and Ni nanowires.[13,44] Moreover, there are few examples of aligning the nanowires dispersed in a polymer by a magnetic field.[44]

This paper is the first report about the transparency and electrical conductivity of a composite film, which was obtained by preparing a CCNW dispersed polymethyl methacrylate solution and bar-coating the solution over a glass substrate. Moreover, the result of the alignment control of the CCNWs by application of a magnetic field is also reported.

2. EXPERIMENTAL SECTION

Formation of CCNWs. The CCNW used as a filler was prepared by the electrolytic reduction of hexaamminecobalt(III)chloride according to the method described in the literature.[36] It is already known that the as-grown CCNW consists of cobaltous hydroxide, metallic cobalt, and a low oxidation state cobalt compound according to the electrochemical measurements and various microanalyses.[36,37] An aqueous solution containing 19 mM hexaamminecobalt(III)chloride and 0.1 M of Li_2SO_4 was used as the electrolyte. This aqueous solution was poured into a two-compartment type three-electrode electrolytic cell. The working electrode of the indium-tin-oxide (ITO) glass and the counter electrode of a platinum plate were soaked in the main section of the electrolytic cell. On the other hand, the agar bridge was placed in the other section, and it was electrically connected to a saturated calomel (SCE, TOA Electoronics HC-205C) reference electrode. The soaking area of the working electrode in the electrolyte was 1.0 × 1.0 cm^2. The electrolytic cell was placed in a thermostatted bath, and the electrolysis temperature was maintained at 18 °C. A grayish black thin film consisting of a large amount of CCNW was obtained by applying a potential of −1.03 V vs SCE to the ITO substrate using a potentiostat (HOKUTO DENKO, model HAB-151). The applied quantity of electricity was 2.0 C/cm^2. After the electrolysis, the deposited film was removed from the sample solution, and then washed with water in order to remove the cobalt complex and supporting electrolyte.

Preparation of Composite Films. The CCNWs were mixed with the polymer solution as follows: Polymethyl methacrylate (PMMA, Acros Organics, average molecular weight 35000) was used as the polymer. The PMMA solution was obtained by mixing PMMA with methylethylketone (weight ratio = 1:10). The CCNWs, which were carefully scraped from the ITO substrate, were added to the above-mentioned polymer solution. The dispersed solution was then stirred for tens of minutes using a stirrer. After the CCNW had been uniformly dispersed, a part of the dispersed solution was removed, and applied to the substrate by the bar-coating method. After its application, it was dried for one hour at 60 °C, and the composite film was obtained. The typical film thickness was 5 μm. The thickness of the film was measured using a surface profile measuring system (Sloan Co., model Dektak 3030). The visible light transmittance and electric conductivity of the composite film were measured. The visible light transmittance was measured by an ultraviolet−visible spectrophotometer (HITACHI U-3000). The electric conductivity was measured in two directions; i.e., perpendicular to the film surface ($\sigma_\perp$) and parallel to the film surface ($\sigma_{//}$). As for the measurement in the direction of the film thickness, the composite film was formed on a Cu substrate (lower electrode), and then a thin Au film (upper electrode, 3 mm × 3 mm) was vacuum deposited by a vacuum deposition method on the composite film in order to make a sandwich-structured cell.[45] The electric conductivity in the direction of the film thickness was then measured by the four-terminal method according to the method described in the literature.[45] The power source was a Kikusui Electronics Co. model PAB70−1A. The electric current flowing at a voltage of 0.8 V was measured by an electrometer (Advantest Co., model R8240). The interelectrode voltage was measured by a digital multimeter (Keithley, model 195A). As for the measurement in the direction parallel to the film surface, a composite film was formed on a glass substrate, and then a pair of comb-like structured Au electrodes was deposited in a vacuum on the surface of the composite film in order to make a planar cell. The details of the shape of the electrode, the interelectrode distance, the length of the electrode, etc., were previously reported.[34] The current−voltage characteristic was measured using the previously mentioned electrometer and power source, and the electric conductivity was calculated. The morphology of the CCNW and the composite film was observed using a scanning electron microscope (SEM, Topcon ABT-32), an optical microscope (Saitoh Kougaku Co., model SKM-3100B-PC), and a laser microscope (Keyence VK-9700 microscope).

Magnetic Alignment of CCNWs. As for the method of aligning the CCNW in a given direction, the substrate was placed between two ferrite magnet plates (flux density: 100 mT) immediately after the composite film was formed on the substrate by the bar coating method (before the solvent completely vaporized). The alignment control of the CCNW was examined for the cases when the magnetic field was applied in the directions perpendicular to the composite film surface and when it was applied parallel to the surface. The flux density was checked using a tesla meter (Kanetec Co., model TM-701).

3. RESULTS AND DISCUSSION

Dispersibility of CCNWs. Figure 1 shows the optical micrograph (a) and SEM image (b) of the CCNW deposit, which was electrochemically formed on the ITO substrate by the method described in the Experimental Section. A large amount of the CCNW with an average diameter of 400 nm and an average length of 45 μm is coagulated to form a grayish black film (applied electric charge: 2.0 C/cm^2). Figure 2, part A, shows a micrograph of the PMMA films, which contains the dispersed CCNW of 0.53% by weight (a), 1.86% (b), 3.61% (c), and 6.86% (d). Part B shows a photograph of the PMMA film with each dispersion amount (film thickness: 5 μm). The substrate is a glass plate. Though it cannot be visually observed that the CCNWs are included in the PMMA film, it can be observed using an optical microscope that the nanowires of about 5 to 40 μm in length are dispersed in the composite film. Because the average length of the as-grown CCNW formed on the ITO is 45 μm (Figure 1B), it is presumed that the CCNWs were cut during the operation of scraping them from the ITO or of dispersing them into the PMMA solution. It can be seen from Figure 2A that there are two cases for the state of the nanowire; one is that each nanowire separately exists, and the other is that several nanowires exist in an aggregation state. The CCNWs are easily dispersed into the polymer solution by only stirring as described in the Experimental Section. As for the reasons for the high dispersibility of the CCNWs, it can be presumed that the main surface component of the CCNWs is cobaltous hydroxide and a low-oxidation state cobalt compound, and that it has a high chemical compatibility with a general-purpose polymer having polar groups. Therefore, there is no concern of strong flocculation, which is often observed when using carbon nanotubes, etc., and is a major concern in

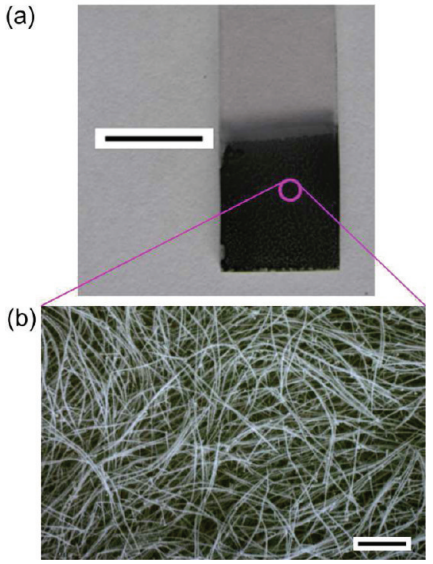

Figure 1. (a) Photograph and (b) SEM image of the cobalt compound nanowires (CCNWs) prepared on the ITO by passing a charge (Q) of 2.0 C/cm^2. Scale bars in parts a and b are 1 cm and 10 μm, respectively.

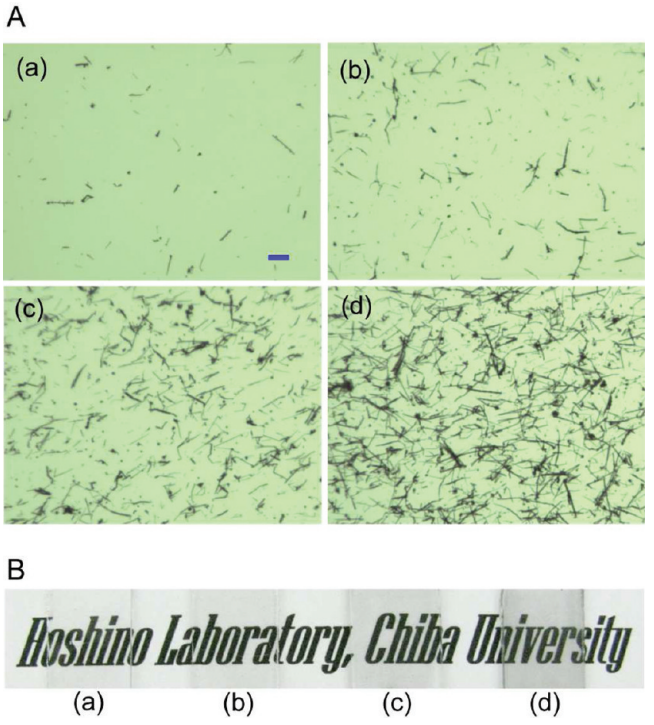

Figure 2. (A) Optical micrographs of the PMMA composite films containing (a) 0.53, (b) 1.86, (c) 3.61, and (d) 6.86 wt % CCNW. The scale bar in panel a corresponds to 20 μm and is applied to panels b–d. (B) Corresponding photographs of the composite films a–d in part A. The films were formed on a glass plate. Scale bar: 1 cm.

forming a composite film; therefore, a special dispersing device and process are unnecessary.

Characterization of Composite Films. Figure 3 shows the results of the permeability measurement on the PMMA composite film. Curve a indicates the visible light transmission of the

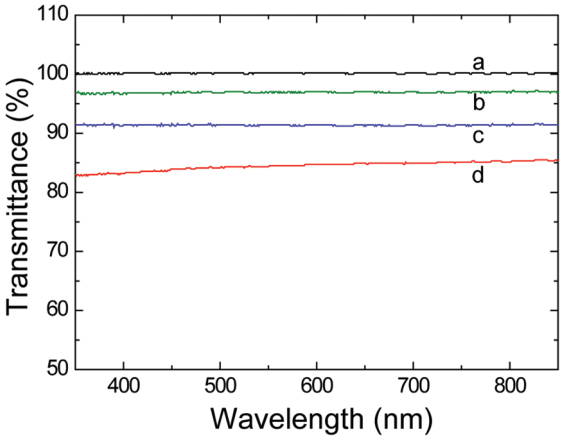

Figure 3. Transmission spectra of the composite films (5 μm thick, coated on a glass plate) containing (b) 0.74, (c) 3.04, and (d) 4.79 wt % CCNW. (a) Spectrum of a PMMA single film.

PMMA-only film, which does not contain the CCNW, and this value is almost 100%. Curve b, which indicates the visible light transmission of the composite film containing 0.74 wt % CCNW in the PMMA, exhibited a very high permeability of about 97%. The visible-light transmission decreased as the weight fraction (x) of the CCNWs increased. Even so, it can be seen that the transmission exceeded 80% when x was ca. 5 wt %.

Next, the electric conductivity of the composite film in a direction perpendicular to the film surface $\sigma_\perp$ and the one in a parallel direction to the film surface $\sigma_{//}$ was examined. Figure 4, part A, shows the relation between $\sigma_\perp$ and x. The value of $\sigma_\perp$ dramatically increased by 9 orders of magnitude even at a very low percolation threshold of $x = 5.3 \times 10^{-3}$ (0.53 wt %). The electric conductivity ($\sigma_\perp$) of the polymer nanocomposite film in which the nanowires were dispersed strongly depended on the value of the volume fraction p and aspect ratio (length to diameter) L/d of the nanowire. $\sigma_\perp$ is given by eq 1 according to the percolation theory.

$$\sigma_\perp = \sigma_0(p - p_c)^t \quad (p \geq p_c) \tag{1}$$

where σ_0 is an extrapolation value to 100 vol % of the volume fraction of the CCNWs, and it corresponds to the electric conductivity of the CCNWs aggregate. p_c is the percolation threshold of the filler, and it is the volume fraction at the transition from an insulator to a conductor. t is a critical exponent. p_c is expressed by the following eq 2 or 3 using L/d according to the concept of the excluded volume.[6]

$$p_c \approx 1/(2L/d) \tag{2}$$

$$p_c \approx 0.7/(L/d) \tag{3}$$

To apply eq 1, the weight fraction x plotted on the X-axis in Figure 4A is converted into a volume fraction p using eq 4,[46] and the data were plotted again (curve a in Figure 4B). ρ_{CCNW} and ρ_{PMMA} indicate the densities of CCNW and PMMA, respectively. The value of ρ_{CCNW} was set assuming that the CCNW consists only of $Co(OH)_2$, and that its density was equal to that of $Co(OH)_2$ (3.597 g/cm^3).[47] As for the value of ρ_{PMMA}, the value of 1.19 g/cm^3 in the literature was used.[48]

$$p = \frac{x\rho_{PMMA}}{\rho_{CCNW} + x(\rho_{PMMA} - \rho_{CCNW})} \tag{4}$$

dx.doi.org/10.1021/am200260v |ACS Appl. Mater. Interfaces 2011, 3, 2341–2348

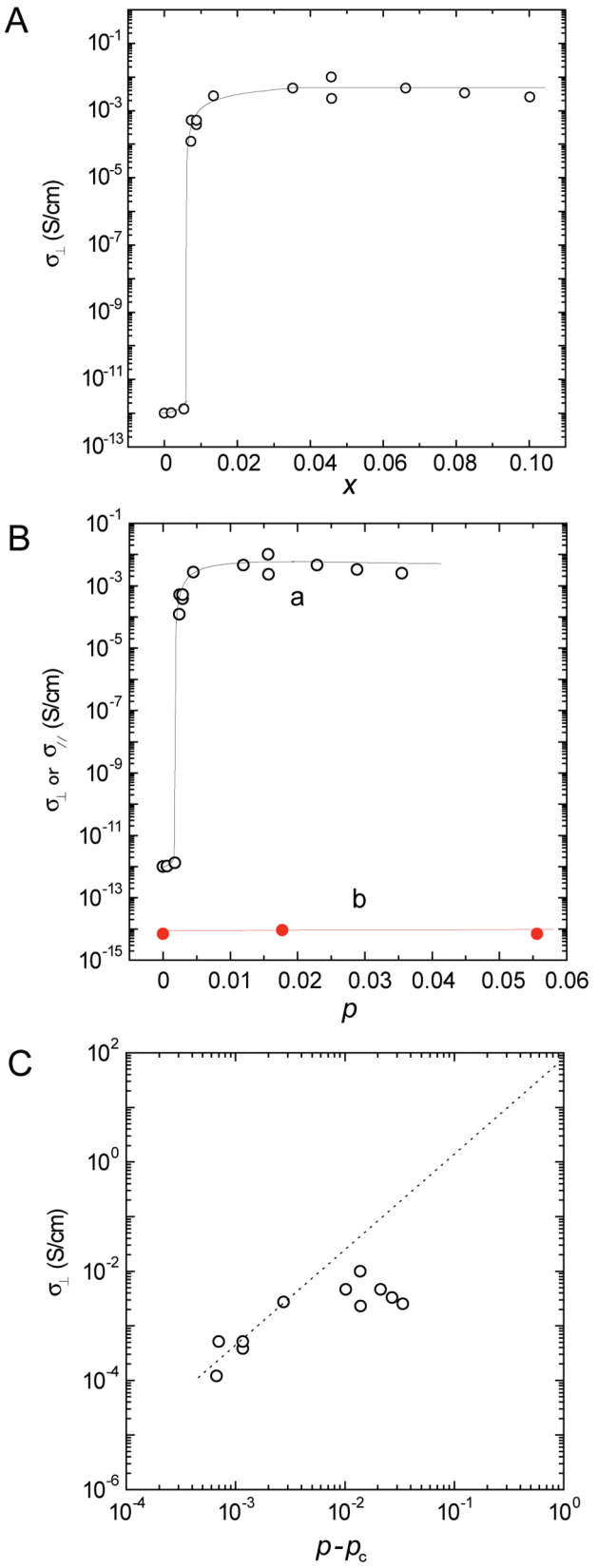

Figure 4. (A) Logarithm of $\sigma_\perp$ plotted as a function of the weight fraction of CCNW, x, for the PMMA composite films. (B) Dependence of the logarithm of (a) $\sigma_\perp$ and (b) $\sigma_{//}$ on the volume fraction of CCNW, p. (C) Plot of log $\sigma_\perp$ and log$(p - p_c)$ for the composite films with p above the percolation threshold, p_c.

The value of $\sigma_\perp$ for the composite film dramatically increased by 9 orders of magnitude at the very low percolation threshold of 0.18 vol%. It is important to use a nanofiller having a low percolation threshold from an engineering aspect because the nanofiller is usually more expensive than the polymer matrix. The value of p_c = 0.18 vol % is almost equivalent to the percolation threshold of the PMMA/carbon nanotube composite system,[6] and it is expected that this nanocomposite has a high degree of technological utility. However, we should note that space resolution is one of the key requirements for display applications. At $p = p_c$ (see image a in Figure 2A), the composition uniformity can be lost as the testing area becomes smaller than ca. 40 × 40 μm^2. The maximum testing area, s, is nearly inversely proportional to p: p = 0.62% (image b in Figure 2A), s = 22 × 22 μm^2; p = 1.22% (image c in Figure 2A), s = 15 × 15 μm^2; p = 2.38% (image d in Figure 2A), s = 10 × 10 μm^2. Figure 4, part C, shows the relation between log $\sigma_\perp$ and log$(p - p_c)$. The range in which the plot bears a linear relationship, that is, the plot apparently obeys eq 1, was limited to the low dispersion amount range of $p - p_c \leq 2.8 \times 10^{-3}$. The value of σ_0 obtained by extrapolating the line in this range to $p - p_c = 1$ was 59 S/cm. On the other hand, the electric conductivity of a piece of CCNW was measured to be 6.7×10^{-3} S/cm at a bias voltage of 0.80 V by the method cited in the literature.[49] This deviation implies that our PMMA composite films, in which a wire length exceeds the film thickness, do not strictly obey the percolation theory. Untereker et al.[50] prepared some polyurethane composite films containing conductive filler particles and found that the maximum conductivity was only the order of 1% of that of the bulk conductive materials. This was interpreted to mean that the electric conductivity of the composites is intrinsically limited by the impedance of contact between the filler particles. However, the maximum conductivity of our PMMA composite films (see Figure 4A or curve a in Figure 4B) was comparable to the conductivity of the single CCNW, 6.7×10^{-3} S/cm. This inconsistency may be again explained by the specific feature of the PMMA composite system, i.e., the number of contact between the fillers in our system is likely much less than that in the ordinary system which obeys the percolation theory. The critical exponent t calculated from the inclination of the linear plot was 1.7 ± 0.5, which was a value intermediate between the t value of the 2D system (t = 1.3) and the one for the 3D system (t = 2).[6,8,13] The mean values of d and L of the CCNW were 400 nm and 22 μm, respectively. Consequently, the value of p_c calculated by eqs 2 and 3 are 9.1×10^{-3} and 1.3×10^{-2}, respectively. The p_c value of 1.8×10^{-3}, which was estimated from Figure 4B, is considerably smaller than the expected values. Since the mean length (22 μm) of the CCNW is greater than the film thickness (5 μm), we expected that there was no threshold p_c in the change of $\sigma_\perp$, and that $\sigma_\perp$ monotonously increased along with an increase in p. However, contrary to our expectations, the existence of a threshold indicates that both surfaces of the film cannot be electrically connected by only one CCNW piece. That is, it indicates that more than at least two CCNW pieces were required for the connection. When compared to a system having the same aspect ratio and a shorter wire length compared to the film thickness, it is easily imagined that p_c become small in the CCNW system having a wire length that exceeds the film thickness. Furthermore, the cause of the low p_c can be explained by assuming a weak interaction between the CCNWs.[51] When such an interaction exists, it is expected that the spatial distribution of the nanowires does not become random during the solvent evaporation process as the film dries. As a result, it is

presumed that a conduction pass is formed with a lower dispersion concentration compared to the case when the CCNWs were completely distributed at random. In the region of $p - p_c \geq 2.8 \times 10^{-3}$, the value of $\sigma_\perp$ deviated from the value expected from eq 1, and was almost saturated. The following two reasons can be considered as the causes. The first reason is that an electric conduction network in the high dispersion region is formed with the CCNW bundles rather than an individual CCNW piece as understood from the result shown in Figure 2A. That is, in this case, since the newly added CCNWs do not effectively contribute to the electric conduction, a lower electric conductivity than the value expected from the extrapolated percolation fit will be indicated. The second reason is that the electric conduction may be inhibited by the presence of PMMA between the electrode (Au layer) and CCNW. Kim et al.[7] found that though a polymer-rich layer was formed on the surface of the film when multilayer carbon nanotubes were dispersed into the PMMA film, the electric conductivity was increased by 2 orders of magnitude when the layer was mechanically scraped.

Though the value of the electric conductivity $\sigma_\perp$ in the direction of the film thickness of the PMMA-only film is 1.0×10^{-12} S/cm as indicated in the plot ($p = 0$ wt %) of Figure 4B, the conductivity $\sigma_{//}$ in the direction parallel to the film surface was 7.0×10^{-15} S/cm. The reason why the value of $\sigma_{//}$ was lower than the value of $\sigma_\perp$ is that the effect of the interface resistance between the electrode and film was included.[35] Curve b in Figure 4B shows the relation between $\sigma_{//}$ and p, and it was found that the value of $\sigma_{//}$ did not depend on the value of p in the examined range of p, and that it was about 1×10^{-14} S/cm. This indicates that the composite film became an anisotropic conduction layer, which was nonconductive in the direction parallel to the surface though it indicated a conductivity in the direction of the film thickness in the range of $p \geq 1.8 \times 10^{-3}$. As confirmed from the optical micrograph shown in Figure 2A, the CCNWs did not mutually come in contact, and the electrically conducting path was not formed in a direction parallel to the film surface.

Alignment Control of CCNWs in a Magnetic Field. Because the CCNW mainly consists of $Co(OH)_2$ and Co that are magnetic,[52] the CCNW can be expected to have a magnetic orientation effect. A magnetic field was then applied to the composite film according to the Experimental Section. Figure 5 shows laser microscope photographs of the composite film surfaces: (a) the magnetic field was not applied, (b) the magnetic field was applied perpendicular to the film surface, and (c) the magnetic field was applied parallel to the film surface. The 3D display corresponding to each photograph is indicated on the right of each photograph. x and p of this composite film are 1.2×10^{-1} and 4.2×10^{-2}, respectively. When the magnetic field was applied perpendicular to the film surface (b), the CCNW aligned perpendicular to the film surface. Also, the length of the protruding part was almost equal to the length (10−15 μm), which was obtained by subtracting the film thickness (5 μm) from the length of the CCNW. When the magnetic field was not applied (a), there were some slightly bloated portions on the surface of the film, and the nanowires showed a tendency to be obliquely aligned in the direction of the film thickness. However, when the magnetic field was applied parallel to the film surface, no bloated portion was observed, which suggested that the nanowires were aligned parallel to the film surface. In order to confirm this, the specimen, which was prepared by applying a magnetic field parallel to the film surface, was observed using an optical microscope. Figure 6 shows the optical micrograph of the

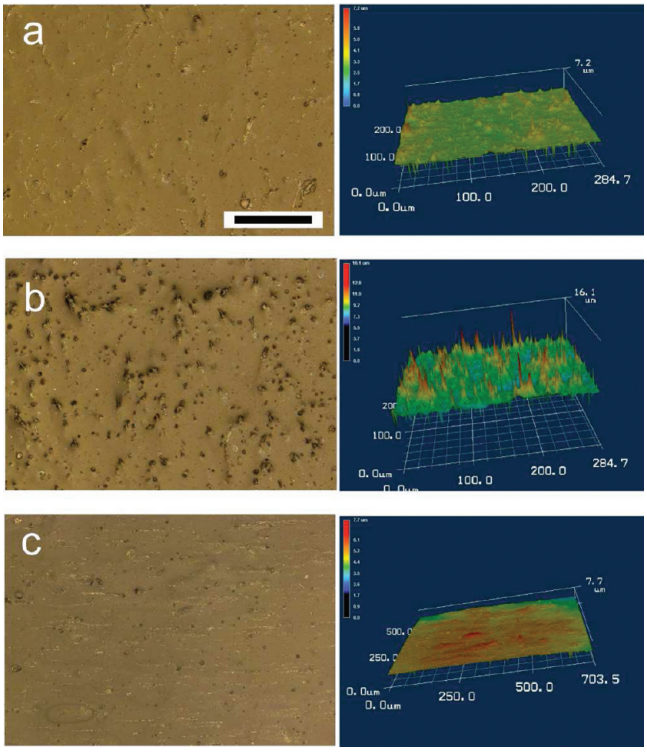

Figure 5. Laser microscopic surface images of random and aligned PMMA composite films. (a) CCNWs are randomly distributed in the film. The right-hand side image shows the corresponding 3D surface morphology of the film. (b) CCNWs are aligned perpendicular to the film surface. (c) CCNWs are aligned parallel to the film surface. The x and p values of the films were 1.2×10^{-1} and 4.2×10^{-2}, respectively. The scale bar in panel a corresponds to 50 μm and is applied to panels b and c.

composite films: (a) the magnetic field was applied in a direction parallel to the direction in which the bar was dragged during the production of the film (arrow in figure), and (b) the magnetic field was applied perpendicular to the direction in which the bar was dragged. The specimens in panels c and d were, respectively, prepared by applying a magnetic field perpendicular to the film surface, and without applying the magnetic field. The values of x and p of the composite film were 1.2×10^{-1} and 4.2×10^{-2}, respectively. As can be seen from photographs a and b, the direction of the long axis of the CCNW was along the direction of the applied magnetic field, and did not depend on the direction in which the bar was dragged. It was found that the CCNWs were aligned parallel to the magnetic field since its length was 5−40 μm. Moreover, the results of images c and d support the results of Figure 5, and it was cofirmed that the former was in a state of perpendicular alignment, and that the latter was in a state of nonalignment.

Next, the $\sigma_\perp$ values of the above-mentioned perpendicular aligned film, parallel-aligned film, and nonaligned film were measured, and these results are shown in Table 1. The values of x and p of the PMMA composite film were 4.6×10^{-2} and 1.6×10^{-2}, respectively. The $\sigma_\perp$ value of the perpendicular aligned film was about seven times that of the nonaligned film. The reason for this may be explained by assuming that the CCNW, which had not contributed to the electric conduction in the direction perpendicular to the film surface, was able to contribute to the electric conduction by the alignment effect of the magnetic field. For instance, CCNWs, such as the one obliquely aligned in the

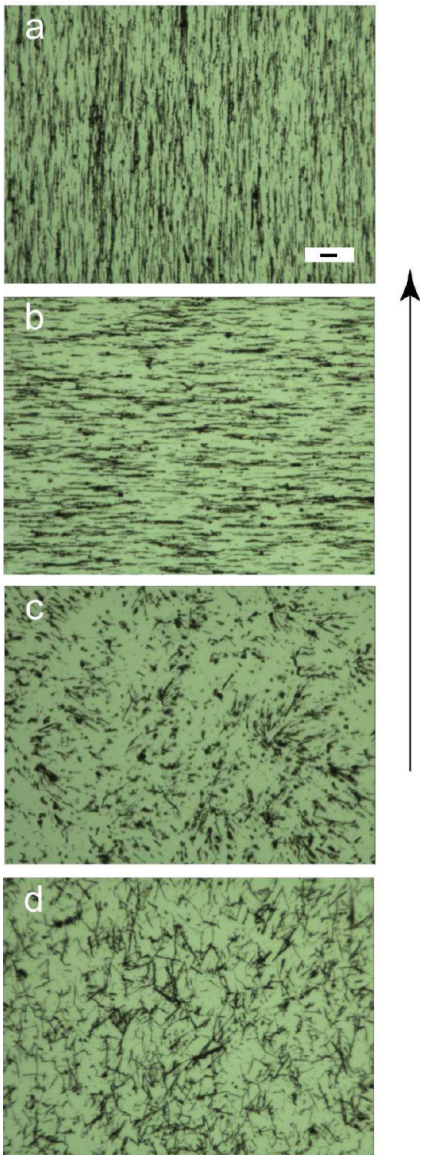

Figure 6. Optical micrographs of the aligned and random state composite films. (a, b) Surface images indicating the films prepared in a magnetic field (100 mT) applied parallel and perpendicular to the bar coating direction, respectively. (c) Image where the magnetic field was applied perpendicular to the film surface. (d) Film prepared under no magnetic field. The x and p values of the films were 1.2×10^{-1} and 4.2×10^{-2}, respectively. The arrow indicates the direction of the bar coating. The scale bar in panel a corresponds to 20 μm and is applied to panels b–d.

Table 1. Electric Conductivities ($\sigma_\perp$) of PMMA Composite Films[a] Treated in and without a Magnetic Field[b]

film	$\sigma_\perp$ (S/cm)
vertically aligned composite film (in magnetic field)	2.0×10^{-2}
parallel-aligned composite film (in magnetic field)	2.1×10^{-12}
nonaligned composite film (without magnetic field)	2.8×10^{-3}

[a] $p = 1.6 \times 10^{-2}$ and $x = 4.5 \times 10^{-2}$. [b] 100 mT.

direction of the film thickness, but does not penetrate through the upper surface and the lower side of the film, and the one forming the bundle can be assumed. The value of $\sigma_\perp$ for the parallel-aligned film was on the order of 1×10^{-12}, which indicated a nonconductivity. This is attributed to the decreased probability of the continuous contact of wires in the direction perpendicular to the film surface due to the alignment of the wires in a direction parallel to the film surface. These results indicate the possibility of controlling the electric conductivity perpendicular to the film surface by application of a magnetic field, and the development of an application for AFC can be expected. White et al.[53] presented a three-dimensional simulation of electrical conductivity for networks containing conductive, finite-sized rods as a function of axial orientation. They revealed that the simulated electrical conductivity displays a maximum at slight uniaxial orientation, which is less pronounced at higher volume fractions and aspect ratios of rods, and that the electrical conductivity decreases as the rods become highly aligned due to the decrease in the intersection probability of adjacent rods. This is inconsistent with the result in Table 1 in which $\sigma_\perp$ for the vertically aligned film is larger than that for the nonaligned film. The inconsistency should be based on the specific feature of the PMMA/CCNW composite system in which much intersection of the CCNW is not necessary condition for the electrical conduction along the film thickness.

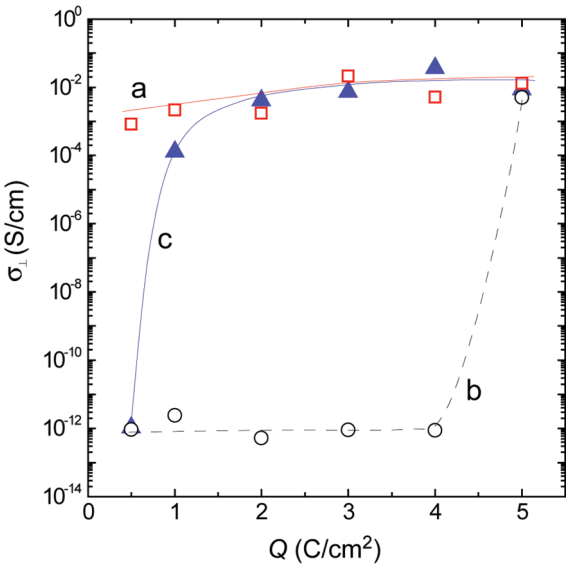

Figure 7. Dependence of $\sigma_\perp$ on Q for the PMMA composite films prepared under magnetic fields applied (a) perpendicular and (b) parallel to the film surfaces. (c) Dependence of the films prepared under no magnetic field. The values of x and p were 3.6×10^{-2} and 1.2×10^{-2}, respectively.

The average length L of the CCNWs dispersed in the PMMA film was changed along with a change in the applied quantity of the electricity Q during the electrosynthesis. The values of L at Q = 0.50, 1.0, 2.0, 3.0, and 4.0 C/cm^2 were 11, 20, 22, 26, and 27 μm, respectively. Figure 7 shows the relation between $\sigma_\perp$ and Q of the nanocomposite film for (a) vertical alignment to the film surface, (b) parallel alignment, and (c) nonalignment. The p value of the PMMA composite film was selected as the constant value of 1.2×10^{-2}. When a treatment without the application of a magnetic field was done (c), under the condition of Q = 0.50 C/cm^2 (L = 11 μm), the electric conductivity in a direction perpendicular to the film surface did not appear though the average length of the long axis of the CCNW was about twice the film thickness. This indicates that the value of p_c of the CCNW at

$L = 11\ \mu$m is greater than 1.2×10^{-2}. The electric conductivity appeared in the range of $Q \geq 1.0$ C/cm^2. The electric conductivity appeared under the condition of $Q = 0.50$ C/cm^2 ($L = 11\ \mu$m) when the CCNWs were aligned perpendicular to the film surface (a). The reason for this is attributed to the disappearance of the percolation threshold due to the penetration of a CCNW piece through the film. When the CCNWs were aligned parallel to the film surface, it was found that the electric conductivity did not appear in the range of $Q \leq 4.0$ C/cm^2, but if the value of Q exceeded this range, the electric conductivity appeared. This is attributed to the significant change in the shape of the CCNW at $Q = 4.0$ C/cm^2 (see the Supporting Information).[37] That is, during the electrolytic treatment up to 2.0 C/cm^2, the shape of the CCNW was almost unchanged and only increased in length. However, when Q exceeded 2.0 C/cm^2, a needle-shaped structure appeared on the surface of the nanowire, and when Q exceeded 4.0 C/cm^2, the needles fused with one another and an aggregate of nanowires was formed. It can be considered that this aggregate penetrated through the film, and that the electric conductivity appeared.

4. CONCLUSIONS

We presented the characterization results of transparent electrically conductive polymer films in which CCNWs were dispersed. The CCNWs having an average diameter of 400 nm, average length of 22 μm and electric conductivity of 6.7×10^{-3} S/cm were dispersed in a PMMA solution by simply stirring, and the CCNW dispersing polymer film of 5 μm thickness was successfully prepared on a substrate by the bar coating method. The electric conductivity threshold existed though the average length of the CCNW exceeded the film thickness. The volume fraction of the CCNW at the threshold was 0.18 vol %. The electric conductivity of 5×10^{-3} S/cm and spectral transmittance of 92% were achieved at a volume fraction of 1 vol %. The CCNWs were aligned by applying a relatively weak magnetic field (100 mT) using ferrite magnets. It was found that the electric conductivity in a direction perpendicular to the film surface depended on the alignment direction of the CCNWs and increased in the following order: a film with the CCNWs aligned parallel to the film surface < a film with nonaligned CCNWs < a film with the CCNWs aligned perpendicular to the film surface. The above-described low electric conduction percolation threshold, high visible-light transmission, electric conductivity tunable characteristic by the nanowire alignment, and flexible nature will make the CCNW-dispersed transparent film attractive for use in flexible electronics.

■ ASSOCIATED CONTENT

Ⓢ Supporting Information. SEM images of CCNWs prepared by passing various amount of electricity. This material is available free of charge via the Internet at http://pubs.acs.org.

■ AUTHOR INFORMATION

Corresponding Author

*Fax: +81-43-290-3478. E-mail: k_hoshino@faculty.chiba-u.jp.

■ ACKNOWLEDGMENT

This work was partially supported by a grant from the Iketani Science and Technology Foundation, Japan.

■ REFERENCES

(1) Granqvist, C. G.; Hultåker, A. *Thin Solid Films* **2002**, *411*, 1–5.
(2) Kumar, A.; Zhou, C. *ACS Nano* **2010**, *4*, 11–14.
(3) Minami, T.; Miyata, T. *Thin Solid Films* **2008**, *517*, 1474–1477.
(4) Minami, T. *Thin Solid Films* **2008**, *516*, 5822–5828.
(5) Minami, T. *Thin Solid Films* **2008**, *516*, 1314–1321.
(6) Bauhofer, W.; Kovacs, J. Z. *Compos. Sci. Technol.* **2009**, *69*, 1486–1498.
(7) Kim, D. O.; Lee, M. H.; Lee, J. H.; Lee, T.-W.; Kim, K. J.; Lee, Y. K.; Kim, T.; Choi, H. R.; Koo, J. C.; Nam, J.-D. *Org. Electron.* **2008**, *9*, 1–13.
(8) Al-Saleh, M. H.; Sundararaj, U. *Carbon* **2009**, *47*, 2–22.
(9) Ajayan, P. M.; Stephan, O.; Colliex, C.; Trauth, D. *Science* **1994**, *265*, 1212–1214.
(10) Spitalsky, Z.; Tasis, D.; Papagelis, K.; Galiotis, C. *Prog. Polym. Sci.* **2010**, *35*, 357–401.
(11) O'Connor, I.; De, S.; Coleman, J. N.; Gun'ko, Y. K. *Carbon* **2009**, *47*, 1983–1988.
(12) Lin, B.; Gelves, G. A.; Haber, J. A.; Pötschke, P.; Sundararaj, U. *Macromol. Mater. Eng.* **2008**, *293*, 631–640.
(13) Lonjon, A.; Laffont, L.; Demont, P.; Dantras, E.; Lacabanne, C. *J. Phys. Chem. C* **2009**, *113*, 12002–12006.
(14) Pei, Q.; Zuccarello, G.; Ahlskog, M.; Inganäs, O. *Polymer* **1994**, *35*, 1347–1351.
(15) Groenendaal, L.; Jonas, F.; Freitag, D.; Pielartzik, H.; Reynolds, J. R. *Adv. Mater.* **2000**, *12*, 481–494.
(16) Louwet, F.; Groenendaal, L.; Dhaen, J.; Manca, J.; Lupppen, J. V.; Verdonck, E.; Leenders, L. *Synth. Met.* **2003**, *135−136*, 115–117.
(17) Lindell, L.; Burquel, A.; Jakobsson, F. L. E.; Lemaur, V.; Berggren, M.; Lazzaroni, R.; Cornil, J.; Salaneck, W. R.; Crispin, X. *Chem. Mater.* **2006**, *18*, 4246–4252.
(18) Crispin, X.; Jakobsson, F. L. E.; Crispin, A.; Grim, P. C. M.; Andersson, P.; Volodin, A.; van Haesendonck, C.; Van der Auweraer, M.; Salaneck, W. R.; Berggren, M. *Chem. Mater.* **2006**, *18*, 4354–4360.
(19) Xia, Y.; Ouyang, J. *ACS Appl. Mater. Interfaces* **2010**, *2*, 474–483.
(20) Heras, A.; Colina, A.; López-Palacios, J.; Kaskela, A.; Nasibulin, A. G.; Ruiz, V.; Kauppinen, E. I. *Electrochem. Commun.* **2009**, *11*, 442–445.
(21) Dan, B.; Irvin, G. C.; Pasquali, M. *ACS Nano* **2009**, *3*, 835–843.
(22) Ki, H. S.; Yeum, J. H.; Choe, S.; Kim, J. H.; Cheong, I. W. *Compos. Sci. Technol.* **2009**, *69*, 645–650.
(23) Song, Y. I.; Yang, C.-M.; Kim, D. Y.; Kanoh, H.; Kaneko, K. *J. Colloid Interface Sci.* **2008**, *318*, 365–371.
(24) Schrage, C.; Kaskel, S. *ACS Appl. Mater. Interfaces* **2009**, *1*, 1640–1644.
(25) De, S.; Higgins, T. M.; Lyons, P. E.; Doherty, E. M.; Nirmalraj, P. N.; Blau, W. J.; Boland, J. J.; Coleman, J. N. *ACS Nano* **2009**, *3*, 1767–1774.
(26) Hu, L.; Kim, H. S.; Lee, J.-Y.; Peumans, P.; Cui, Y. *ACS Nano* **2010**, *4*, 2955–2963.
(27) Azulai, D.; Belenkova, T.; Gilon, H.; Barkay, Z.; Markovich, G. *Nano Lett.* **2009**, *9*, 4246–4249.
(28) Kang, M.-G.; Park, H. J.; Ahn, S. H.; Guo, L. J. *Sol. Energy Mater. Sol. Cells* **2010**, *94*, 1179–1184.
(29) Hong, T.-K.; Lee, D. W.; Choi, H. J.; Shin, H. S.; Kim, B.-S. *ACS Nano* **2010**, *4*, 3861–3868.
(30) Wang, S. J.; Geng, Y.; Zheng, Q.; Kim, J.-K. *Carbon* **2010**, *48*, 1815–1823.
(31) Tian, L.; Meziani, M. J.; Lu, F.; Kong, C. Y.; Cao, Li.; Thorne, T. J.; Sun, Y.-P. *ACS Appl. Mater. Interfaces* **2010**, *2*, 3217–3222.
(32) Lee, H.; Rajagopalan, R.; Robinson, J.; Pantano, C. G. *ACS Appl. Mater. Interfaces* **2009**, *1*, 927–933.
(33) Shim, B. S.; Zhu, J.; Jan, E.; Critchley, K.; Kotov, N. A. *ACS Nano* **2010**, *4*, 3725–3734.
(34) Hoshino, K.; Yazawa, N.; Tanaka, Y.; Chiba, T.; Izumizawa, T.; Kubo, M. *ACS Appl. Mater. Interfaces* **2010**, *2*, 413–424.
(35) Miyazaki, T.; Kim., S.-K.; Hoshino, K. *Chem. Mater.* **2006**, *18*, 5302–5311.

(36) Hoshino, K.; Hitsuoka, Y. *Electrochem. Commun.* **2005**, *7*, 821–828.
(37) Asano, Y.; Komatsu, T.; Murashiro, K.; Hoshino, K. *J. Power Sources* **2011**, *196*, 5215–5222.
(38) Lee, S.-W.; Hama, M.-H.; Kar, J. P.; Lee, W.; Myoung, J.-M. *Microelectron. Eng.* **2010**, *87*, 10–14.
(39) Lee, S.-W.; Jeong, M.-C.; Myoung, J.-M.; Chae, G.-S.; Chung, I.-J. *Appl. Phys. Lett.* **2007**, *90*, 133115.
(40) Hangarter, C. M.; Myung, N. V. *Chem. Mater.* **2005**, *17*, 1320–1324.
(41) Bentley, A. K.; Trethewey, J. S.; Ellis, A. B.; Crone, W. C. *Nano Lett.* **2004**, *4*, 487–490.
(42) Tanase, M.; Silevitch, D. M.; Hultgren, A.; Bauer, L. A.; Searson, P. C.; Meyer, G. J.; Reicha, D. H. *J. Appl. Phys.* **2002**, *91*, 8549–8551.
(43) Tanase, M.; Bauer, L. A.; Hultgren, A.; Silevitch, D. M.; Sun, L.; Reich, D. H.; Searson, P. C.; Meyer, G. J. *Nano Lett.* **2001**, *1*, 155–158.
(44) Park, J.-M.; Kim, S.-J.; Yoon, D.-J.; Hansen, G.; DeVries, K. L. *Compos. Sci. Technol.* **2007**, *67*, 2121–2134.
(45) Koshikawa, H.; Usui, H.; Maekawa, Y. *J. Membr. Sci.* **2009**, *327*, 182–187.
(46) Kota, A. K.; Cipriano, B. H.; Duesterberg, M. K.; Gershon, A. L.; Powell, D.; Raghavan, S. R.; Bruck, H. A. *Macromolecules* **2007**, *40*, 7400–7406.
(47) In *The Merck Index*; Budavari, S., Ed.; Merck & Co.: Whitehouse Station, NJ, 1996; pp 413−414.
(48) In *Lange's Handbook of Chemistry*; Dean, J. A., Ed.; McGraw-Hill: New York, 1979; pp 7−454.
(49) de Pablo, P. J.; Graugnard, E.; Walsh, B.; Andres, R. P.; Datta, S.; Reifenberger, R. *Appl. Phys. Lett.* **1999**, *74*, 323–325.
(50) Untereker, D.; Lyu, S.; Schley, J.; Martinez, G.; Lohstreter, L. *ACS Appl. Mater. Interfaces* **2009**, *1*, 97–101.
(51) Murphy, R.; Nicolosi, V.; Hernandez, Y.; McCarthy, D.; Rickard, D.; Vrbanic, D.; Mrzel, A.; Mihailovic, D.; Blau, W. J.; Coleman, J. N. *Scr. Mater.* **2006**, *54*, 417–420.
(52) Li, L.; Qian, H.; Ren, J. *Chem. Commun.* **2005**, 4083–4085.
(53) White, S. I.; DiDonna, B. A.; Mu, M.; Lubensky, T. C.; Winey, K. I. *Phys. Rev. B* **2009**, *79*, 024301.